

# Illumination induced charge separation at tetraphenyl-porphyrin/metal oxide interfaces

Y. Zidon and Yoram Shapira

*Department of Physical Electronics, Faculty of Engineering, Tel-Aviv University, Ramat-Aviv 69978, Israel*

Th. Dittrich<sup>a)</sup>

*Hahn-Meitner-Institute, Glienicke Strasse 100, 14109 Berlin, Germany*

(Received 4 July 2007; accepted 16 July 2007; published online 6 September 2007)

Charge separation processes were studied at tetraphenyl-porphyrin (H<sub>2</sub>TPP)/metal oxide interfaces by surface photovoltage spectroscopy. The thickness of the depleted Ti and Sn oxide layers was about 2 nm. Acceptorlike interface states play a crucial role in the steady-state light-induced negative charging of H<sub>2</sub>TPP surface layers as well as in tunneling or light-induced discharging. The results indicate that steady-state negative charging of the H<sub>2</sub>TPP layer is induced by preferential recombination of holes at the (H<sub>2</sub>TPP)/metal oxide interface and depends only weakly on temperature. The modulated surface photovoltage is dominated by hole transport at low temperatures and by electron transport at higher temperatures. The activation energy of the latter is of the order of 0.4 eV. © 2007 American Institute of Physics. [DOI: 10.1063/1.2777200]

## INTRODUCTION

Understanding the charge separation processes in conducting organic layer/metal oxide interfaces is essential since metal oxides are used as conducting transparent electrodes in organic optoelectronics devices<sup>1</sup> and as semiconducting substrates in organic-based sensors and solar cells.<sup>2</sup> In order to understand the basic charge separation processes and exciton dissociation paths, a deeper understanding of the interface electronic structure is needed. Due to the very low drift velocities, which are usually of the order of  $10^{-3}$ – $10^{-7}$  cm<sup>2</sup>/V s,<sup>3</sup> insight into the charge transport properties is also essential for subsequent charge separation.

Organic/metal interfaces are fairly well studied. Charge exchange at the interface results in interface dipoles and a band bending at the interface in some systems.<sup>4,5</sup> Interfaces with metal oxides introduce additional complexity, so charge transfer between the organic layers and the substrate surface states has to be considered. Additionally, mainly oxygen, but also metal atoms, may diffuse from the substrate to the organic film, altering the interface electronic structure.<sup>6,7</sup> Nakanishi *et al.*<sup>8</sup> found that electron transfer from the conducting polymer to indium tin oxide (ITO), In<sub>2</sub>O<sub>3</sub>, and SnO<sub>2</sub> substrates occurred at the interfaces. Although the origin of this electron transfer is not clear, the authors speculate that the surface states of the substrate play a major role. This result suggests that metal oxide substrates characteristically attract electrons out of the conducting polymers without the application of an electric field and interfacial band bending may be formed.<sup>9</sup> Moreover, electron transfer at these interfaces is enhanced at higher temperatures. The exact interface electronic structure is not fully understood. For instance, it is not clear whether the Fermi levels of the conducting metal oxide and the organic highest occupied molecular orbital<sup>9</sup>

(HOMO) are aligned or whether alignment exists within the HOMO-LUMO (lowest unoccupied molecular orbital) gap.<sup>10,11</sup>

Charge separation mechanisms at interfaces with thin conducting layers can be characterized at high sensitivity by surface photovoltage spectroscopy (SPS) using a Kelvin Probe (KP).<sup>12</sup> Few SPS studies characterized the charge separation at organic layer/metal oxide (H<sub>2</sub>TPP/metal oxide) interfaces,<sup>13,14</sup> all of them using common inorganic physical concepts, such as surface and interface band bending, to explain the observed surface photovoltage (SPV) signal. Recently, we showed the complexity of analyzing the SPV signal of organic thin layers.<sup>15,16</sup> The obtained surface photovoltage at the interfaces of thin free-base tetraphenylporphyrin (H<sub>2</sub>TPP) and Au is a summation of two main SPV mechanisms, i.e., internal photoemission from the Au substrate and exciton dissociation at the H<sub>2</sub>TPP interface. However, the point that organic layers might need a different SPS analysis than the classic for inorganic semiconductor is not fully stressed for metal oxide/organic interfaces.

In this study, charge separation processes at interfaces between H<sub>2</sub>TPP and SnO<sub>2</sub>:F (denoted by FTO) or TiO<sub>2</sub> substrates are characterized using SPS and KP transients at different temperatures and ambients. H<sub>2</sub>TPP is synthetic porphyrin derivative with several absorption bands: the Soret band around 2.9 eV and the Q bands at about 2.4, 2.2, 2.1, and 1.9 eV.<sup>17</sup> The 1.9 eV transition is considered as the HOMO-LUMO optical band gap. Since all the H<sub>2</sub>TPP transitions are below the TiO<sub>2</sub> and the FTO band gaps, charge transfer to the organic layer that may follow the band-to-band transition in the substrate is avoided.<sup>18</sup>

## EXPERIMENT

Organic H<sub>2</sub>TPP layers (thickness 75 nm) were evaporated (sublimation temperature:<sup>19</sup> 588 K) on glass substrates coated with a conducting oxide layer (SnO<sub>2</sub>:F, resistance:

<sup>a)</sup>Electronic mail: dittrich@hmi.de

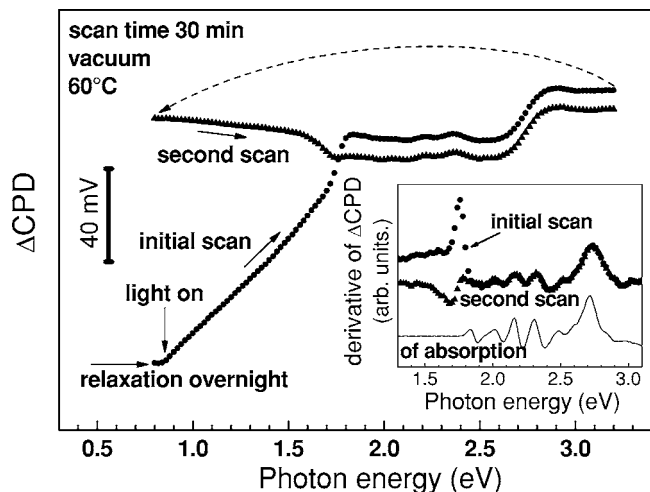


FIG. 1. Contact potential difference spectra for  $\text{H}_2\text{TPP}/\text{SnO}_2:\text{F}$  measured at  $60^\circ\text{C}$  in vacuum, with the initial scan taken after relaxation overnight in the dark and the second scan immediately after the initial scan. The inset compares the derivatives of both spectra with that of the absorption spectrum.

$10\ \Omega/\square$ ) and on polished Ti foils coated with a thermal Ti oxide layer (the thickness of the  $\text{TiO}_2$  layer was about 2 nm). For optical absorption measurements, a  $\text{H}_2\text{TPP}$  layer was evaporated on a bare glass substrate. The substrates were cleaned ultrasonically in acetone and isopropanol, and dried in  $\text{N}_2$  before evaporation in high vacuum at room temperature. The deposition rate of the  $\text{H}_2\text{TPP}$  (5,10,15,20-tetraphenyl-21H, 23H-porphine, Sigma Aldrich, Inc.) layers was set to about  $1\ \text{\AA}/\text{s}$ . The samples were stored in high vacuum after evaporation and between measurements.

Spectrum-dependent light-induced charge separation was investigated by SPS with a Kelvin probe (Besocke Delta Phi) and a quartz prism monochromator (SPM2). A 250 W halogen lamp was used for illumination. The measurements were performed in high vacuum at temperatures up to  $210^\circ\text{C}$  and in air. The SPS technique monitors light-induced changes of the work function difference between the sample and a vibrating gold grid. The work function of the vibrating gold grid is assumed to be independent of illumination. Therefore, the measured light-induced work function difference corresponds to the light-induced changes in the contact potential difference ( $\Delta\text{CPD}$ ) of the sample, which is the negative SPV. The resolution time of the measurement technique is of the order of 1 s, depending on the integration time constant of the lock-in amplifier in the Kelvin probe controller. A full SPV spectrum was measured within about 30 min. A red light emitting diode (LED) was used for time-dependent measurements of  $\Delta\text{CPD}$ .

## RESULTS AND DISCUSSION

### Surface photovoltage spectra

Figure 1 shows the spectra of the contact potential difference for  $\text{H}_2\text{TPP}/\text{FTO}$  measured at  $60^\circ\text{C}$  in vacuum. The initial spectrum (denoted as the initial scan) was measured after overnight relaxation in the dark. The next spectrum (denoted as the second scan) was obtained just after completion of the initial spectrum. The spectrum of the third scan

was practically identical to the second one. The slit of the monochromator was opened after three points of the spectrum that were measured in the dark. After opening the slit of the monochromator, the contact potential difference started to increase immediately. The increase of  $\Delta\text{CPD}$  points to a light-induced increase of negative charge near the surface of the sample, which is treated as negative charging of the  $\text{H}_2\text{TPP}$  layer within this work. The value of  $\Delta\text{CPD}$  is further increased between 1.7 and 1.8 eV, at the onset of the HOMO-LUMO gap absorption. Absorption peaks related to transitions into  $Q_x(1,0)$ ,  $Q_y(0,0)$ , and  $Q_y(1,0)$ , denoted here for simplicity as  $Q_2$ ,  $Q_3$ , and  $Q_4$  transitions, in the  $\text{H}_2\text{TPP}$  layer can be identified at 2.05, 2.21, and 2.36 eV, respectively. The value of  $\Delta\text{CPD}$  increases again strongly with the onset of the absorption related to transitions into the Soret band of the  $\text{H}_2\text{TPP}$ .

After resetting the photon energy of the exciting light back to 0.8 eV,  $\Delta\text{CPD}$  decreased by about 10 mV, which was not significant in comparison to the value obtained after overnight relaxation in the dark. Well into the second scan,  $\Delta\text{CPD}$  continued to decrease due to ongoing discharging of the  $\text{H}_2\text{TPP}$  layer. At photon energies of about 1.5 eV, the discharging process became more significant, indicating that discharge of the  $\text{H}_2\text{TPP}$  layer can be assisted by light with photon energies higher than about 1.5 eV. The discharge of the  $\text{H}_2\text{TPP}$  stopped abruptly at the photon energy corresponding to the absorption threshold due to HOMO-LUMO transitions in the  $\text{H}_2\text{TPP}$  layer.

The shapes of the initial and second scans were identical at photon energies higher than 1.9 eV. This can be clearly seen if the derivatives of both spectra are compared with each other (inset of Fig. 1). The peaks of the derivatives related to the  $Q_2$ ,  $Q_3$ ,  $Q_4$ , and Soret transitions are in excellent agreement with those of the derivative of the absorption spectrum. The peak of the  $Q_1$  transition [ $Q_x(0,0)$ ] is masked by charging and discharging processes that can be related to the influence of interactions with interface states at organic/metal oxide heterojunctions.<sup>6–8</sup>

The kinetics of charging and discharging of the  $\text{H}_2\text{TPP}$  layer below the HOMO-LUMO transition strongly depend on the temperature. This is demonstrated by the  $\Delta\text{CPD}$  spectra shown in Fig. 2 for the second scans of the  $\text{H}_2\text{TPP}/\text{FTO}$  sample. At lower temperatures, the light-assisted discharging dominates the  $\Delta\text{CPD}$  spectra at photon energies below 1.7 eV, whereas negative charging takes place at higher temperatures (above  $140^\circ\text{C}$ ). This shows that the discharging process of the  $\text{H}_2\text{TPP}$  layer accelerates with increasing temperature.

In air, the  $\text{H}_2\text{TPP}$  layer is negatively charged even after relaxation overnight (see spectra in Fig. 3). The  $\Delta\text{CPD}$  spectra are quite similar for  $\text{H}_2\text{TPP}/\text{FTO}$  and  $\text{H}_2\text{TPP}/\text{TiO}_2/\text{Ti}$  samples. However, in vacuum, the  $\Delta\text{CPD}$  spectra of the  $\text{H}_2\text{TPP}/\text{TiO}_2/\text{Ti}$  are more smeared out, i.e., changes in the  $\text{TiO}_2$  surface states become dominant. It was found that surface states related to oxygen vacancies at  $\text{TiO}_2$  surfaces were passivated in air<sup>20</sup> and low electron injection yields were obtained at  $\text{TiO}_2$  interfaces.<sup>21</sup> In air, the light-assisted discharging process starts at photon energies of about 1.4 eV ( $\text{H}_2\text{TPP}/\text{FTO}$ ) or 1.3 eV ( $\text{H}_2\text{TPP}/\text{TiO}_2/\text{Ti}$ ) and stops

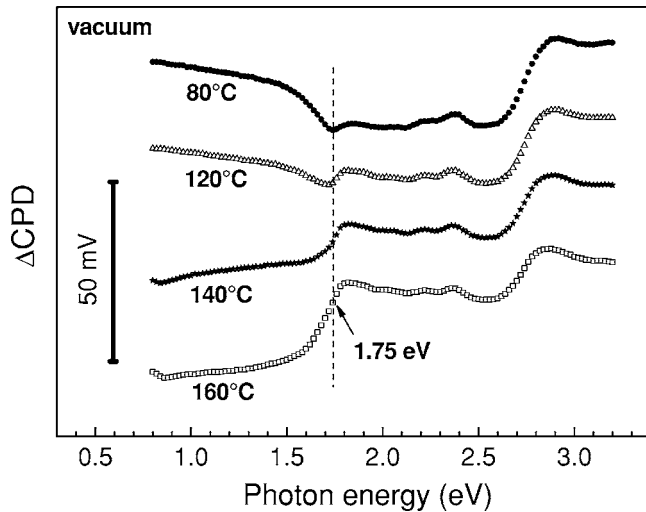


FIG. 2. Contact potential difference spectra for  $\text{H}_2\text{TPP}/\text{SnO}_2:\text{F}$  measured in vacuum at different temperatures, taken as second scans (see Fig. 1).

abruptly when the HOMO-LUMO transition sets in. For  $\text{H}_2\text{TPP}/\text{TiO}_2/\text{Ti}$ , the light-induced changes of  $\Delta\text{CPD}$  are stronger than for  $\text{H}_2\text{TPP}/\text{FTO}$  and the characteristic features of the  $Q_2$ ,  $Q_3$ ,  $Q_4$ , and Soret transitions are not as well pronounced. Additional transitions may appear (e.g., the additional discharging at photon energies of about 2 eV).

The type of doping cannot be explicitly determined from these SPS measurements since charging processes in the organic layer cannot be treated simply as charge separation in a depletion layer. Charge separation is also determined by illumination and ambient induced internal potential distribution<sup>15</sup> as well as by charge separation mechanisms. Thus, interface states play a key role in charging and discharging of the  $\text{H}_2\text{TPP}$  surface layer. It is practically impossible to avoid any permanent charging during the spectroscopy measurements, and the light-induced charging rather than thermodynamic equilibrium built-in fields is mainly deduced from the SPS data of organic/metal oxides interfaces.

### Negative charging and discharging mechanisms

Acceptorlike surface states (negatively charged when populated) are assumed at the metal oxide surfaces. On the

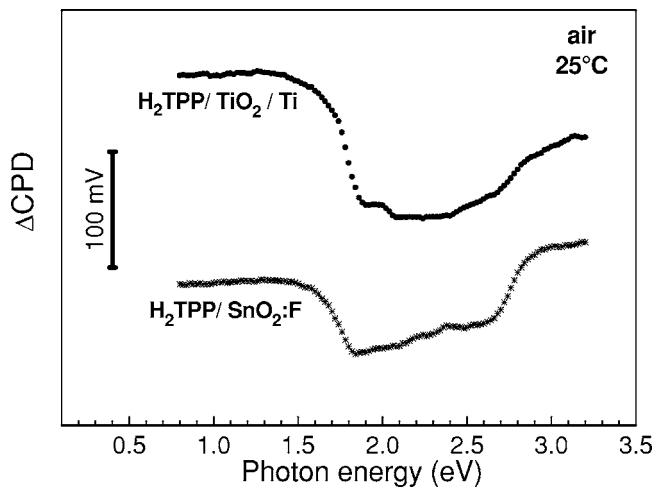


FIG. 3. Contact potential difference spectra for  $\text{H}_2\text{TPP}/\text{TiO}_2/\text{Ti}$  and  $\text{H}_2\text{TPP}/\text{SnO}_2:\text{F}$  measured at 25 °C in air, taken as initial scans.

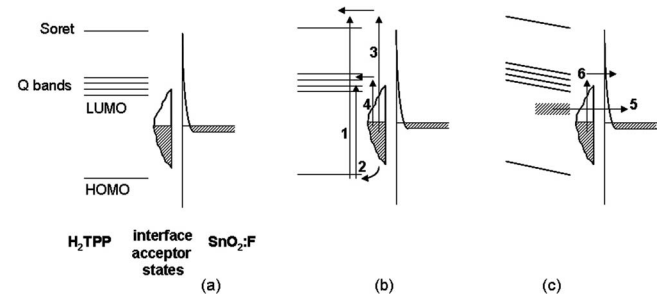


FIG. 4. Schematic band diagram of (a) the system consisting of  $\text{H}_2\text{TPP}$  layer, interface states, and very thin depleted metal oxide layer with a metal contact, (b) processes of light-induced negative charging due to generation in the  $\text{H}_2\text{TPP}$  layer and preferential recombination of holes at the interface (1, 2) and due to generation from interface states (3, 4), and (c) discharging processes of the negatively charged  $\text{H}_2\text{TPP}$  layer due to tunneling via interface states (5) and due to light-assisted injection of electrons from interface states into the metal oxide (6).

one hand, the surface states interact with the metal or the highly conductive electrode via a very thin layer so that tunneling is possible. On the other hand, due to charge exchange at the interface, the surface states are also coupled to the  $\text{H}_2\text{TPP}$  layer. This situation is sketched in Fig. 4(a). The initial scan of the  $\text{H}_2\text{TPP}/\text{FTO}$  sample shows that surface charging can occur already at photon energies in the near infrared region. The negative charging is enhanced at photon energies of about 1.5–1.6 eV. The initial negative charging is related to surface states– $Q$  bands transitions and, probably, the enhanced charging is the transition to the Soret band, the higher absorption band. The Soret band transition onset is at about 2.6 eV. Therefore, these observations indicate that the surface Fermi level position is, at most, about 1 eV above the HOMO level of the  $\text{H}_2\text{TPP}$ .

If Fermi level alignment exists at the interface, then the 1 eV value may indicate the Fermi level energy position in the  $\text{H}_2\text{TPP}$  layer. The Fermi level was estimated at about 0.6 eV above the HOMO level of  $\text{H}_2\text{TPP}$  by Harima *et al.*<sup>22</sup> Additionally, a 0.8 eV gap between the HOMO level and the Fermi level of a Au substrate was measured assuming Fermi level alignment at the  $\text{H}_2\text{TPP}/\text{Au}$  interface.<sup>15</sup> Therefore, it is reasonable to deduce that the Fermi level–HOMO gap is less than 1 eV. Due to the broad distribution of interface states, the measurement sensitivity, charging effects, and competing SPV mechanisms, it is difficult to estimate the HOMO–Fermi level gap at the  $\text{H}_2\text{TPP}/\text{FTO}$  interface from the SPV spectra.

During illumination with photon energies above the HOMO-LUMO gap, negative charging is induced by dissociation of excitons at the  $\text{H}_2\text{TPP}/\text{metal oxide}$  interface and preferential recombination of holes at surface states [processes 1 and 2 in Fig. 4(b)]. At lower photon energies, negative surface charging is also possible due to electron injection from interface states into  $\text{H}_2\text{TPP}$  [processes 3 and 4 in Fig. 4(b)]. Simultaneously, photoelectrons can also be injected from interface states into the metal oxide [process 6 in Fig. 4(c)]. The change of the net charge depends on the change of the transition probability of electrons from interface states into the  $\text{H}_2\text{TPP}$ , which depends on the amount of accumulated negative charge in the  $\text{H}_2\text{TPP}$  layer and on the

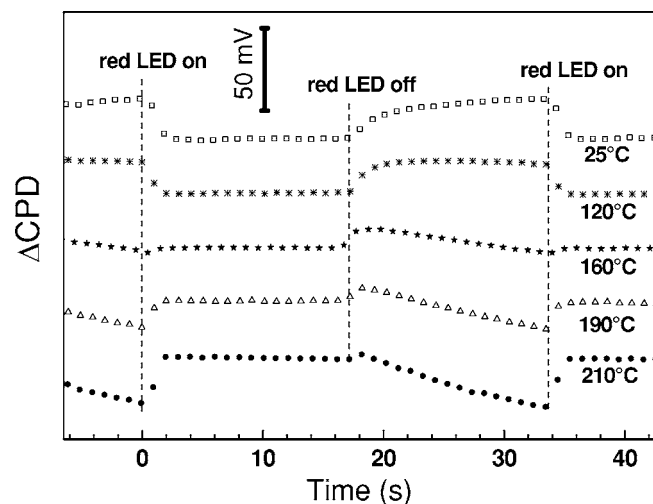


FIG. 5. Contact potential differences as a function of time for  $H_2TPP/FTO$  measured at different temperatures in the dark and under illumination with a red LED.

local field distribution. For example, oxygen is a known acceptorlike dopant,<sup>9</sup> and negatively charged oxygen dominates the field distribution of  $H_2TPP$  deposited in air. Electron transfer from surface states into the metal oxide drives discharging processes. Besides this light-induced discharging process, thermally assisted tunneling should also be considered as a discharging process driven by electrons from polaronic states in the  $H_2TPP$  layer via surface states into the metal oxide layer [process 5 in Fig. 4(c).]

### Modulation of hole and electron transport

The red light of the LED used in this work is mainly absorbed by the  $Q_2$  transition in the  $H_2TPP$  layer. Under slow light intensity modulation of the red LED, the  $H_2TPP$  layer is negatively charged. Figure 5 compares the time dependence of the surface  $\Delta CPD$  for  $H_2TPP/FTO$  interfaces measured at different temperatures in the dark and under illumination, with a red LED blinking at about 0.03 Hz. At low temperatures (below 120 °C), the value of  $\Delta CPD$  decreases under illumination, i.e., the modulation of positive charge is detected. This shows that, besides the negative net charging of the  $H_2TPP$  layer, there is a certain probability of the holes to escape from the interface region, where the excitons dissociate. The value of  $\Delta CPD$  saturates within several seconds under illumination, and the light-induced change of  $\Delta CPD$  depends only weakly on the temperature. The discharging process of the positive charge in the dark is significantly slower than the escape of holes from the interface region.

At temperatures above 140 °C, the light-induced  $\Delta CPD$  changes sign, i.e., modulation of negative charging becomes important. However,  $\Delta CPD$  still increases after switching off the light within 1–2 s, and decreases for longer times (overshoot). The further increase of  $\Delta CPD$  after switching off the red LED is caused by the disappearance of positive charge from the  $H_2TPP$  layer, which is much faster than the disappearance of the negative charge. With increasing temperature, the light-induced increase of  $\Delta CPD$  increases and the

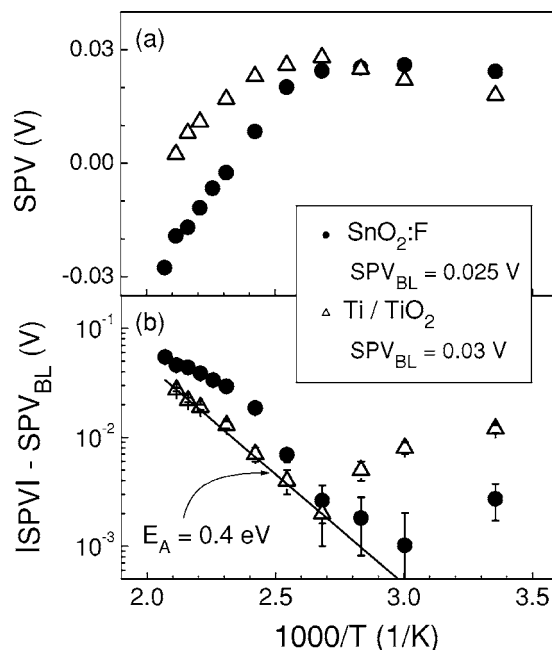


FIG. 6. Temperature dependence of the surface photovoltage signal obtained as (a) the difference of the contact potential difference measured just before the LED was switched on and 4 s after the LED had been switched on, and (b) Arrhenius plots of the surface photovoltage signals corrected to a base line for  $H_2TPP/FTO$  and  $H_2TPP/TiO_2/Ti$ . The modulation frequency of the LED was 0.03 Hz.

overshoot induced by hole recombination decreases. At the same time, the discharging process in the dark becomes much faster with increasing temperature. The overall amount of modulated positive charge decreases with increasing temperature because the recombination rate increases with temperature. Furthermore, the electron transfer from the  $H_2TPP$  towards the metal oxide layer is thermally activated. It is interesting to note that the value of  $\Delta CPD$  saturates within 2 s, which is much shorter than the discharging time. The observation that saturation is reached after 2 s at any temperature suggests that the charge separation processes takes place mainly in close proximity to the interface and not at the front surface. This observation is consistent with the findings of Harima *et al.*<sup>22</sup> who reported that the time response SPV for a given organic/oxidized metal interface is similar to that of a photovoltaic cell having the corresponding organic/metal junction.

The modulated SPV signal can be obtained from the  $\Delta CPD$  measurement as a function of time under the 0.03 Hz illumination modulation ( $SPV = CPD_{light} - CPD_{dark}$ ). The temperature dependence of the SPV signal is shown in Fig. 6(a) for the  $H_2TPP/FTO$  and  $H_2TPP/TiO_2/Ti$  samples. For the  $H_2TPP/FTO$  sample, the SPV changes sign from about +30 to -30 mV between 120 and 210 °C. For the  $H_2TPP/TiO_2/Ti$  sample, the SPV increases with increasing temperature (up to about 120 °C) and decreases with further increasing temperature. However, the sign of the SPV does not change for the  $H_2TPP/TiO_2/Ti$  sample.

Activation energies of dominant processes may be estimated if a common base line is considered. For the sake of simplicity, it is assumed that the positive charging is independent of temperature and that negative charging increases



with increasing temperature. Therefore, the base line is taken at about 30 mV. The resulting Arrhenius plots are shown in Fig. 6(b). For the H<sub>2</sub>TPP/TiO<sub>2</sub>/Ti sample, there is a single thermally activated process at the higher temperatures with an activation energy of about 0.4 eV. For the H<sub>2</sub>TPP/FTO sample, there are at least two thermally activated processes with activation energies of about 0.2 and 0.5 eV, respectively. The origin of the activation energies is not clear at present. The higher activation energy may be related to transport phenomena, since the minimum energy for the formation of a pair of separated free electron and hole was found to be at least 0.4 eV<sup>23</sup>, but it may also be due to discharging effects.

## CONCLUSIONS

Negative charging of H<sub>2</sub>TPP layers strongly affects their SPV spectra measured using a Kelvin probe. This is because of the quasi-steady-state nature of the measurements. Unlike classic SPV analysis of inorganic semiconductors, the illumination induced charging rather than any built-in fields in the dark can be mainly studied using SPS. For organic layer/metal oxide (H<sub>2</sub>TPP/metal oxide) interfaces, charge exchange through acceptorlike interface states plays an important role in the light-induced charging and discharging processes. The H<sub>2</sub>TPP transitions in the SPV spectra increase as the layer is more negatively charged due to increased hole recombination, mainly at the interface. Below 140 °C, the constant negative charging depends weakly on temperature and only hole transport can be modulated. Above 140 °C, electron transport has a stronger effect as the negative charging can be modulated and the discharging processes are enhanced. Activation energy of about 0.4–0.5 eV has been found, which may be related to transport phenomena. The Fermi level of the FTO substrate is, at most, 1 eV above the HOMO level of H<sub>2</sub>TPP.

## ACKNOWLEDGMENTS

The authors are grateful to the group of Professor A. Zaban for providing the TiO<sub>2</sub>/Ti and FTO substrates. Y.Z. is

grateful to the DAAD for financial support. Y.S. is grateful to Monash University, Melbourne, Australia, where he is currently on sabbatical leave.

- <sup>1</sup>J. Kido and T. Matsumoto, Appl. Phys. Lett. **73**, 2866 (1998).
- <sup>2</sup>F. Lenzmann, J. Krueger, S. Burnside, K. Brooks, M. Gratzel, D. Gal, S. Ruhle, and D. Cahen, J. Phys. Chem. B **105**, 6347 (2001).
- <sup>3</sup>Y. Shirota, J. Mater. Chem. **10**, 1 (2000) and references therein.
- <sup>4</sup>H. Ishii, K. Sugiyama, E. Ito, and K. Seki, Adv. Mater. (Weinheim, Ger.) **11**, 605 (1999).
- <sup>5</sup>T. U. Kampen, Appl. Phys. A: Mater. Sci. Process. **82**, 457 (2006).
- <sup>6</sup>A. S. Komolov, P. J. Møller, J. Mortensen, S. A. Komolov, and E. F. Lazneva, Surf. Sci. **586**, 129 (2005).
- <sup>7</sup>H. Peisert, T. Schwieger, M. Knupfer, M. S. Golden, and J. Fink, Synth. Met. **121**, 1435 (2001).
- <sup>8</sup>N. Nakanishi, K. Tada, M. Onoda, and H. Nakayama, Appl. Phys. Lett. **75**, 226 (1999).
- <sup>9</sup>F. Nuesch, M. Carrara, M. Schaer, D. B. Romero, and L. Zuppiroli, Chem. Phys. Lett. **307**, 311 (2001).
- <sup>10</sup>J. Blochwitz, T. Fritz, M. Pfeiffer, K. Leo, D. M. Allow, and N. R. Armstrong, Org. Electron. **2**, 97 (2001).
- <sup>11</sup>C. Tengstedt, W. Osikowicz, W. R. Salaneck, I. D. Parker, C. H. Hsu, and M. Fahlman, Appl. Phys. Lett. **88**, 053502 (2006).
- <sup>12</sup>L. Kronik and Y. Shapira, Surf. Sci. Rep. **37**, 1 (1999) and references therein.
- <sup>13</sup>E. Moons, A. Goossens, and T. Savenije, J. Phys. Chem. B **101**, 8492 (1997).
- <sup>14</sup>M. Eschle, E. Moons, and M. Gratzel, Opt. Mater. (Amsterdam, Neth.) **9**, 138 (1998).
- <sup>15</sup>Y. Zidon, Y. Shapira, Th. Dittrich, and L. Otero, Phys. Rev. B **75**, 195327 (2007).
- <sup>16</sup>Y. Zidon, Y. Shapira, and Th. Dittrich, Appl. Phys. Lett. **90**, 142103 (2007).
- <sup>17</sup>J.-H. Ha, S. I. Yoo, G. Y. Junga, I. R. Paeng, and Y.-R. Kim, J. Mol. Struct. **606**, 189 (2002).
- <sup>18</sup>A. D. Q. Li and L. S. Li, J. Phys. Chem. B **108**, 12842 (2004).
- <sup>19</sup>R. M. Stephenson and S. Malanowski, *Handbook of the Thermodynamics of Organic Compounds* (Elsevier, New York, 1987).
- <sup>20</sup>V. Duzhko, V. Yu. Timoshenko, F. Koch, and Th. Dittrich, Phys. Rev. B **64**, 075204 (2001).
- <sup>21</sup>A. Huijser, T. J. Savenije, and L. D. A. Siebbeles, Thin Solid Films **208**, 511 (2006).
- <sup>22</sup>Y. Harima, K. Yamashita, H. Ishii, and K. Seki, Thin Solid Films **366**, 237 (2000).
- <sup>23</sup>I. G. Hill, A. Kahn, Z. G. Soos, and R. A. Pascal, Jr., Chem. Phys. Lett. **327**, 181 (2000).